LA-UR- 04- 7511

Approved for public release;
distribution is unlimited.

Title: PIEZO-SENSOR SELF-DIAGNOSTICS USING ELECTRICAL IMPEDANCE MEASUREMENTS

Author(s): GyuHae (NMI) Park, LANL, ESA-WR
Charles R. Farrar, LANL, ESA-WR
Amanda C. Rutherford, LANL, ESA-WR
Amy N. Robertson, LANL, ESA-WR

Submitted to: 2004 INTERNATIONAL CONFERENCE ON ADAPTIVE STRUCTURES AND TECHNOLOGIES, BAR HARBOR, MAINE, OCTOBER 24-27, 2004,

Los Alamos
NATIONAL LABORATORY

Form 836 (10/96)

Submission to the Proceedings of 15th International Conference on Adaptive Structures and Technologies, October 25-27 2004, Bar Harbor, ME.

TITLE: Piezoelectric Active Sensor Self-Diagnostics using Electrical Impedance Measurements

Authors: GyuHae Park
Charles R. Farrar
Amanda C. Rutherford
Amy N. Robertson

Engineering Sciences and Applications
Weapon Response Group
Los Alamos National Laboratory
Los Alamos, NM 87545

ABSTRACT

This paper present the piezoelectric sensor self-diagnostic procedure that performs in-situ monitoring of the operational status of piezoelectric materials (PZT) used for sensors and actuators in structural health monitoring (SHM) applications. The use of active-sensing piezoelectric materials has received considerable attention in the SHM community. A critical aspect of the piezoelectric active-sensing technologies is that usually large numbers of distributed sensors and actuators are needed to perform the required monitoring process. The sensor/actuator self-diagnostic procedure, where the sensors/actuators are confirmed to be functioning properly during operation, is therefore a critical component to successfully complete the SHM process and to minimize the false indication regarding the structural health. The basis of this procedure is to track the changes in the capacitive value of piezoelectric materials resulting from the sensor failure, which is manifested in the imaginary part of the measured electrical admittances. Furthermore, through the analytical and experimental investigation, it is confirmed that the bonding layer between the PZT and a host structure significantly contributes to the measured capacitive values. Therefore, by monitoring the imaginary part of the admittances, one can quantitatively assess the degradation of the mechanical/electrical properties of the PZT and its attachment to a host structure. This paper concludes with an experimental example to demonstrate the feasibility of the proposed sensor-diagnostic procedure.

INTRODUCTION

Structural health monitoring (SHM) techniques based on the use of active-sensing piezoelectric materials have received considerable attention in the structural community. The molecular structure of piezoelectric materials (PZT) produces a coupling between the electrical and mechanical domains. Therefore, this type of material generates mechanical

G. Park, C.R. Farrar, A.C. Rutherford, A.N. Robertson – Engineering Sciences & Applications, Los Alamos National Laboratory, Los Alamos, NM 87545

strain in response to an applied electric field. Conversely, the materials produce electric charges when stressed mechanically. This coupling property allows one to design and deploy an "*active*" and "*local*" sensing system whereby the structure is locally excited by a known input, and the corresponding responses are measured by the same excitation source. Some advantages of these devices are; compactness, light-weight, low-power consumption, ease of integration into critical structural areas, ease of activation through electrical signals, higher operating frequency, and low cost. The employment of a known input also facilitates subsequent signal processing of the measured output data.

A critical aspect of the piezoelectric active sensing technologies is that usually large numbers of distributed sensors and actuators are needed to perform the required monitoring process. In addition, the structures in question are usually subjected to various external loading and environmental conditions that may adversely affect the functionality of SHM sensors and actuators. Most current monitoring systems are not intelligent enough to differentiate signal changes caused by damage from those due to the sensor failures. The piezoelectric sensor/actuator self-diagnostic procedure, where the sensors/actuators are confirmed to be functioning properly during operation, is therefore a critical component to successfully complete the SHM process. Because of the brittle nature of PZT, sensor breakage and degradation of mechanical /electrical properties are the most common types of sensor/actuator failures. In addition, the integrity of bonding between a PZT and a host structure should be maintained and monitored throughout their service lives.

This paper describes a piezoelectric sensor self-diagnostic procedure based on electrical impedance measurements. The basis of this procedure is to track the changes in the capacitive value of piezoelectric materials, which is manifested in the imaginary part of the measured electrical admittances (inverse of impedance). Furthermore, through the analytical and experimental investigation, it is confirmed that the bonding layer significantly modifies the measured electrical admittance. Therefore, by monitoring the imaginary part of the admittances, one can quantitatively assess the breakage or degradation of the mechanical /electrical properties of the PZT sensors and the integrity of the bonding condition between a PZT and a host. The rest of this paper includes the literature survey, description of the proposed sensor diagnostic method, experimental procedure and results, and several issues that can be used as a guideline for future investigation.

PREVIOUS WORKS

From the sensor diagnostic standpoint, the breakage of sensor/actuator can be easily identified if a sensor does not produce any measurable output, or an actuator does not reasonably respond to applied signals. However, if only a small fracture occurs within the materials, the sensors/actuators are still able to produce sufficient performance (with distorted signals before/after the sensor fracture), potentially leading to a false indication on the structural condition. For piezoelectric sensors, the sensor failures are inevitable after extreme natural hazards, such as an earthquake, recognizing the fact that the sensors are usually the most delicate part in structural systems. Furthermore, the mechanical and electrical properties of PZT materials could be gradually degraded over their service lives. This degradation of sensor quality, as well as degradation in bonding integrity, will be especially problematic, if one needs to employ large numbers of sensors/actuators over a long period time and to identify when to replace the sensor/actuator network. To the authors' best knowledge, however, the issues associated with long-term reliability of the PZT sensors

under the real-world operational condition, and the methods and metrics that can be used to assess the degradation of the piezoelectric sensor/actuator quality have not been sufficiently addressed in the literature.

The importance of the bonding integrity between the PZT and a host structure can be understood intuitively. The fundamental assumption in the piezoelectric active-sensing technology is that the sensors and actuators are perfectly bonded to a structure, and the integrity of bonding layer does not change throughout their service lives, which is not the case in real-world applications. For instance, the adhesives used for bonding the PZT patch have a finite service life, usually shorter than the host structure's life-span.

Crawley and De Luis [1], Park et al. [2] and Sirohi and Chopra [3] have demonstrated the effects of the bond layer, referred to as shear lag effect, on the induced strain transfer mechanisms for surface bonded PZT. The shear lag ratio, $\xi=(S_p/S_b - 1)$, where S_p and S_b are the PZT' and the structure's strain, respectively, is defined as in the following equation. In the perfect bonding ($S_p=S_b$), the shear lag ratio is equal or close to zero.

$$\frac{\partial^2 \xi}{\partial x^2} - \Gamma^2 \xi = 0 \tag{1}$$

and

$$\Gamma^2 = \left(\frac{G_s}{Y_p t_s t_c} + \frac{3 G_s w}{Y_b w_b t_b t_c} \right) \tag{2}$$

where G_s is the shear modulus of bonding material, Y_p and Y_b is the Young's modulus of PZT and the structure, respectively, t_s and t_c is the thickness of the bonding layer and PZT, respectively, and w and w_b is the width of PZT and the structure, respectively. Γ is defined as the shear lag parameter. This equation and further analysis indicates that, if the PZT is used as a sensor, the sensing voltage generated by the host structure's strain is less than that of perfectly bonded condition, hence underestimates the strain in the substructure. From the above Equations, one can clearly infer that the shear lag effect, which modifies the PZT sensing and actuation mechanisms, is the function of the geometry and mechanical properties of the PZT (t_c, w, Y_p) and those of bonding materials (t_s, G_s). In order to reduce the shear lag phenomenon, one needs to use higher shear modules adhesives and keep the thickness of the bonding layer as thin as possible, as indicated by Equation (2). The changes in these properties can be considered as the degradation of the bonding quality.

Contrary to the breakage or the degradation of the sensor quality, a great amount of research efforts have been focused on understanding the effects of the bonding layer on the sensor/actuator performance [4,5,6,7,8,9,10,11,12,13,14]. Through experimental and analytical investigation, these studies showed that the effects of bonding defects are remarkable, modifying stress and strain transfer mechanism [5,7,8,11], frequency spectrums including modal frequencies and damping ratio [4,6], the performance of closed-loop vibration control [6,9] and constrained layer damping [12], and measured electrical impedances[10,13].

Although the importance of debonding effects is prevalent, a literature search shows that there exist only a few studies investigating how to assess the quality of the bonding condition. Saint-Pierre et al [15] proposed a new debonding identification algorithm by monitoring the resonance of a PZT measured by electrical impedances. As the de-bonding area between the PZT and the host increases, the shape of the PZT resonance becomes sharper and distinctive, and the magnitudes of the host resonances are reduced. The

essentially same approach was proposed by Giurgiutiu et al [16]. However, because of the mechanical impedance mismatching between the PZT and the host, the method does not show required sensitivity to a small degree of debonding. This method also is not able to account for the sensor breakage that may simultaneously occur with the debonding process, because the sensor breakage would apparently changes the resonance of the PZT. Sun and Tong [17] proposed a closed loop based debonding identification scheme. The premise of the method is to use a sensitive control system that can be destabilized by a slight frequency shift caused by small edge debonding in PZT. Although the method shows the great sensitivity to only 0.1% of debonding in a simulation study, the issues associated with how to differentiate the frequency shift caused by structural damage and that of actuator debonding was not fully addressed.

It is apparent that the importance of sensor self-diagnostic procedures received little attention in literature. In order to fully implement current active-sensing systems in practice beyond proof-of-concept demonstration, the authors believe that an efficient sensor-self diagnostic procedure should be adopted in the SHM process, forming a motivation of this study.

SENSOR SELF-DIAGNOSTICS USING ADMITTANCE MEASUREMENTS

The premise of the proposed sensor self-diagnostic procedure is to track the changes in the imaginary part of the electrical admittance of the PZT. In this section, we theoretically and experimentally demonstrate that the degradation of the mechanical/electrical properties of the PZT sensors and its attachment to the external structure produces measurable changes in PZT's measured admittances.

Piezoelectric transducers acting in the 'direct' manner produce an electrical charge when stressed mechanically. Conversely, a mechanical strain is produced when an electrical field is applied. The effects of piezoelectricity between the electrical and mechanical variables can be described by the following linear relations [18]

$$S_i = s_{ij}^E T_j + d_{mi} E_m \tag{3}$$

$$D_m = d_{mi} T_i + \varepsilon_{mk}^T E_k \tag{4}$$

where S is the mechanical strain, T is the mechanical stress, E is the electric field, D is the charge density, s is the mechanical compliance, d is the piezoelectric coupling constant, ε is the dielectric constant of the PZT, and the subscripts i, j, m and k indicate the direction of stress, strain or electric field. The superscripts E and T indicate that those quantities are measured with electrodes connected together and zero stress, respectively. The first equation describes the converse piezoelectric effect and the second one describes the direct piezoelectric effect.

Differentiating the charge density with respect to time and integrating it over the electroded area yields the total electric current flowing through the PZT. For 1-d case, the electric current of free piezoelectric transducer (I) is calculate from Equation (4), when set to $T = 0$,

$$I = i\omega \iint D_3 dxdy \tag{5}$$

$$= i\omega \iint \varepsilon_{33}^{T}(1-\delta)E_3 dxdy$$

where ω angular frequency, δ is the dielectric loss tangent of the PZT, and x, y is the plane coordinates of a PZT patch. The subscript 3 indicate the charge density is along the z-axis perpendicular to the x-y (1-2) plane. Note that a uniform distribution of the charge density in PZT is assumed in the integration. Then, the electrical admittance of a free PZT transducer, which is defined as the ratio of the energizing voltage to the resulting current, is given in the following relation.

$$Y_{free}(\omega) = \frac{I}{V} = i\omega \frac{wl}{t_c}\left(\varepsilon_{33}^{T}(1-i\delta)\right) \tag{6}$$

where V is the applied voltage, and w, l, t_c is the width, length and thickness of PZT, respectively.

When a PZT is surface-bonded to a structure, Liang et al. [19] shows that the electrical admittance $Y(\omega)$ of the PZT transducer is a combined function of the mechanical impedance of the host structure $Z_s(\omega)$ and that of the PZT actuator $Z_a(\omega)$, in addition to the terms in Equation (6), given by;

$$Y(\omega) = i\omega \frac{wl}{t_c}\left(\varepsilon_{33}^{T}(1-i\delta) - d_{31}^{2}Y_p^E + \frac{Z_a(\omega)}{Z_a(\omega)+Z_s(\omega)} d_{31}^{2}\hat{Y}^E\left(\frac{\tan kl}{kl}\right)\right) \tag{7}$$

where Y_p^E is the complex Young's modulus of the PZT at zero electric field. k, the wave number of the PZT is given by,

$$k = \omega\sqrt{\frac{\rho}{\hat{Y}^E}} \tag{8}$$

where ρ is the mass density of the PZT. The Equation (7) is derived based on an assumption that a PZT patch is attached to one end of a structural system, whereas the other end of the PZT is fixed. This assumption regarding the interaction at two discrete points is consistent with the mechanism of force transfer from the bonded PZT transducer to the structure.

Equation (7) sets groundwork for using the PZT sensors/actuators for impedance-based structural health monitoring applications [20]. Assuming that the mechanical and electrical property of the PZT does not change over the monitoring period of the host structure, Equation (7) clearly shows that the electrical admittance or impedance of the PZT is directly related to the mechanical impedance of the host structure, allowing the monitoring of the host structure's mechanical properties using the measured electrical property.

The proposed sensor diagnostic process is based on Equations (6) and (7). The admittance of a PZT is clearly a function of its geometry constants (w, l, t_c), mechanical property (Y_p^E) and electrical properties (ε_{33}^{T}, d_{31},δ) of the PZT. It is also obvious from the Equations that the changes in these properties are manifested more distinctly in the imaginary part of the electrical admittance. Therefore, the breakage of the sensor and the degradation of the sensor's quality can be identified by monitoring the imaginary part of the electrical admittance. These changes would cause a downward shift in the slope.

Another significance of Equations (6) and (7) is that one can identify the effect of bonding layer on measured electrical admittance. The effect of the bonding layer is obtained by letting $Z_s(\omega)$ be ∞ in Equation (7),

$$Y(\omega) = i\omega \frac{wl}{t_c}\left(\varepsilon_{33}^{T}(1-i\delta) - d_{31}^{2}Y_p^E\right) \tag{9}$$

It is clear from Equations (6) and (9) that the electrical admittance of the same PZT would be different if it is under a free-free condition or surface-bonded (or commonly referred to as blocked) condition. The blocked condition would cause a downward shift in the slope of the electrical admittance of a free PZT with the factor of $d_{31}^{2}Y_p^E$. The assumption, $Z_s(\omega) = \infty$, would be valid, especially at lower frequency range, because the mechanical impedance of the structure in question is usually several orders of magnitude greater than that of a PZT transducer. Even though this derivation does not explicitly consider the parameters of bonding materials such as thickness or shear modulus, it is obvious from Equation (9) that the use of PZT transducer with lower Y_p^E will reduce the effect of the bonding condition on the measured admittance, which is consistent with the shear lag loss, shown in Equation (2).

The following figure shows the measured admittance of free and surface bonded PZTs. The 5A PZT materials with dimensions of 20 x 20 x 0.25 mm are used. The admittances of three free PZT patches were measured in the frequency range of 40-20,000 Hz. These PZTs were then surface-mounted to a thick aluminum beam and plate using an epoxy with vacuum bagging to ensure a better bonding condition, and the admittance measurements were repeated using an Agilent 4294A impedance analyzer.

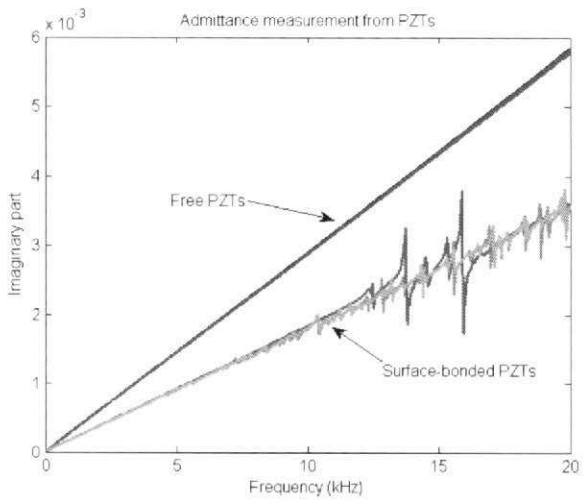

Figure 1: Electrical Admittance Measurement from PZTs under free and surface-bonded conditions

As can be seen in Figure 1, the downward shifting effect of the bonding layer is remarkable. The slope of the imaginary part, which is analogous to the capacitive value of the PZT, was changed from 2.91e-7 to 1.8e-7, resulting in the 38 % reduction. Analytically, it has been however estimated 22 % of a downward shift. It is believed that this discrepancy is coming from the shear modulus of the bonding materials, which is not included in the analysis of Equation (9). The shear modulus of the thin bonding layer may increase the effective Young's modulus of the PZT in Equation (9). In addition, the bonding layer also contains

capacitive dielectric constants connected directly to the PZT in series, resulting in the downward shift of the measured admittance. Therefore, Equation (9) can only be used to qualitatively assess the bonding effect, and more improved modeling, which incorporates the comprehensive electromechanical effects of the bonding layer, would be required for more quantitative estimation of the bonding effects on the measured electrical admittance.

Nevertheless, the importance of this analysis is that the bonding layer contributed to the overall admittance of PZT patches bonded to a structure. Thus, the bonding defects would also affect the measured admittance. Contrary to the sensor breakage, the bonding defects would cause an upward shift in the slope of the imaginary part of the electrical admittance. Therefore, the sensor functionality including the sensor breakage and the degradation of the bonding condition can be assessed by monitoring the imaginary part of the admittances.

It is also important to point out that the changes associated with the sensor functionality are clearly discernible from those of structural damage. Because of capacitive nature of PZT materials, the real part of the admittance/impedance has been mainly used for monitoring in applications. The changes resulting from the structural damage will cause complete changes in real part of the admittance/impedance signatures, while causing variations along the imaginary part of the signatures (no change in the slope). The sensor failures will results in both real and imaginary part of the admittance/impedance signatures, while causing a downward (sensor breakage) and an upward (debonding between PZT transducers and the host) shift in the slope of the imaginary part of the admittance.

To use the proposed sensor diagnostic procedure, one needs measured electrical admittance response data from the PZT, which can be easily accomplished by a simple impedance/admittance measuring circuit [21]. A data acquisition system with higher sampling frequencies would not be necessary because this method is more efficient at lower frequency ranges, up to only several kHz. At higher frequencies, the assumption of $Z_s(\omega) = \infty$ would not be valid, because the mechanical impedance of the PZT becomes comparable to that of the structure. This characteristic will significantly relax the hardware requirement for the proposed sensor diagnostic procedure. Furthermore, just one such device would be needed to check large numbers of sensors and actuators placed in a structure. This proposed method will be very effective in providing a metric that can be used to determine the sensor functionality over a long period of time or after an extreme loading on a structure. The proposed sensor diagnostic procedure can be also useful if one need to check the operational status of a sensing network right after its installation.

EXPERIMENTAL INVESTIGATION

An experiment was performed to check the validity of the proposed concept. Rather than quantitatively assessing the degree of sensor failures, the objectives of this experiment are to determine if the sensors are operating correctly using the proposed sensor diagnostic procedure, for those that are surface-mounted on a structure subjected to extensive impact loadings. This procedure is taken because the control of slight sensor breakages or bonding defects is difficult to obtain experimentally. Controlled projectile impact experiments using the gas gun were conducted on a graphite/epoxy-fiber-reinforced composite plate with surface-bonded PZT transducers. These impacts could be considered as one of operational condition in real-world applications, such as used in unmanned aerial vehicles [22].

Experimental Setup

The test structure is shown in Figure 2. The dimension of the quasi-isotropic composite plate is 609 x 609 x 6.35 mm, whose lay-up contains 48 plies stacked according to the sequence [6(0/45/-45/90)]s using 60% Toray T300 graphite fibers in a 934 Epoxy matrix. Two pairs of piezoelectric (5A) and Macro-Fiber Composite (MFC) patches are mounted on one surface of the plate, as shown in Figure 2. The sizes of the PZT and MFC are 25.4 x 25.4 x 0.254 mm and 25.4 x 12.7 x 0.254 mm, respectively. The MFC are a relatively new type of piezoelectric material that is more flexible than the conventional PZT [23]. The Young's modulus of a flexible MFC is 15 GPa, only a fifth of traditional piezoceramic materials (5A, 66 GPa). As described earlier, MFC is expected to be less affected by the shear lag loss or bonding defects than traditional PZTs because of the lower value in Y_p^E.

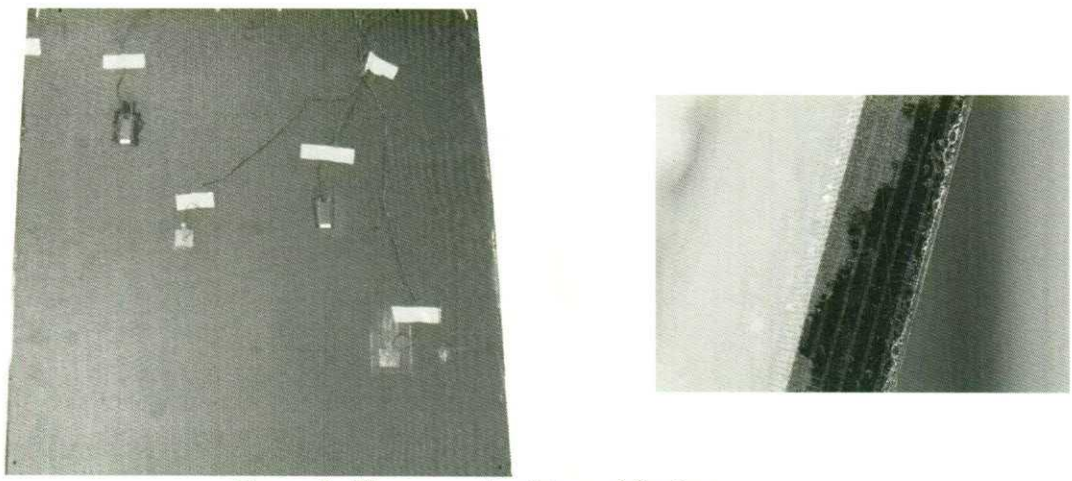

Figure 2: The composite plate used for the test.

In order to measure the electrical admittance of the PZT, a simple impedance measuring circuit was used [21]. The voltage into the PZT is used as the output and the voltage output from the PZT circuit, as seen in Figure 3, is used as the input. V_{out} is proportional to the output current of the PZT. Electrical admittance of the PZT patch is related to the measured input and output voltage of the PZT through the following equation:

$$Y_p = \frac{I}{V} = \frac{V_{out}/R}{V_{in} - V_{out}} \tag{10}$$

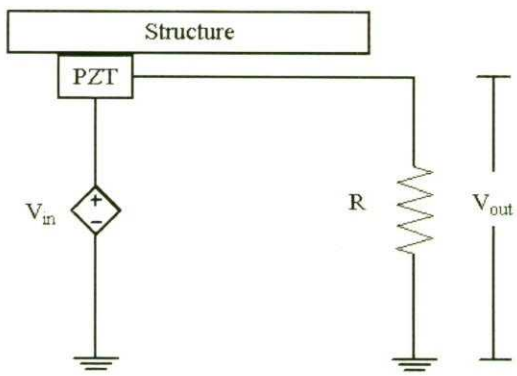

Figure 3: Diagram of PZT circuit indicating locations of measured voltages V_{in} and V_{out}

A commercial data acquisition system controlled from a laptop PC is used to digitize the voltage analog signals at a sampling rate of 51.2 kHz, producing 32,768 time domain data points. An amplified random signal (1 V) is used as the voltage input for the testing. All time history data are first standardized by subtracting the mean and dividing by the standard deviation, as in the following Equation (5).

$$\overline{\mathbf{x}} = \frac{\mathbf{x} - \mu}{\sigma} \tag{11}$$

where $\mathbf{x}$ is the original vector, $\overline{\mathbf{x}}$ is the normalized vector, μ is the mean of the original vector, and σ is the standard deviation of the original vector. This process previously is used to reduce the environmental and operation variability [24]. This process eliminates DC bias and normalizes the variations associated with the differences in excitation levels, which can be caused by changes in the damping of a host structure with respect to temperature variations. Each time history is split up into 29 separate 4096-point blocks, with 75% overlap. A Fast Fourier Transform is then performed on all data blocks in order to transfer the time history information into the frequency domain for the admittance estimate.

A total of 14 baseline measurements with the PZTs and MFCs were recorded to capture environmental variability before the impacts were introduced. The baselines were measured under different ambient and temperature conditions over a three week period. Impact loading is then introduced into the plate by firing a small projectile out of a gas gun. A gas gun is used to propel a 192.3g steel projectile with a spherical nose at the composite plate. Five shots aimed at different locations and at varied velocities (31.09 m/s, 39.93 m/s, 36.88 m/s, 35.66 m/s, 32.92 m/s) created different damage scenarios. The impact locations are shown in relation to the PZT and MFC sensors in Figure 4. No physically visible structural damage was identified during the tests except for Impact 2. Impact 2, with the highest velocity, caused visible damage to the plate. Other impacts, including Impacts 3, 4, and 5, introduced invisible delamination to the plate, which was identified using an ultrasonic C-scan method. The admittance measurements were repeated after each impact to asses the condition of the PZT and MFC.

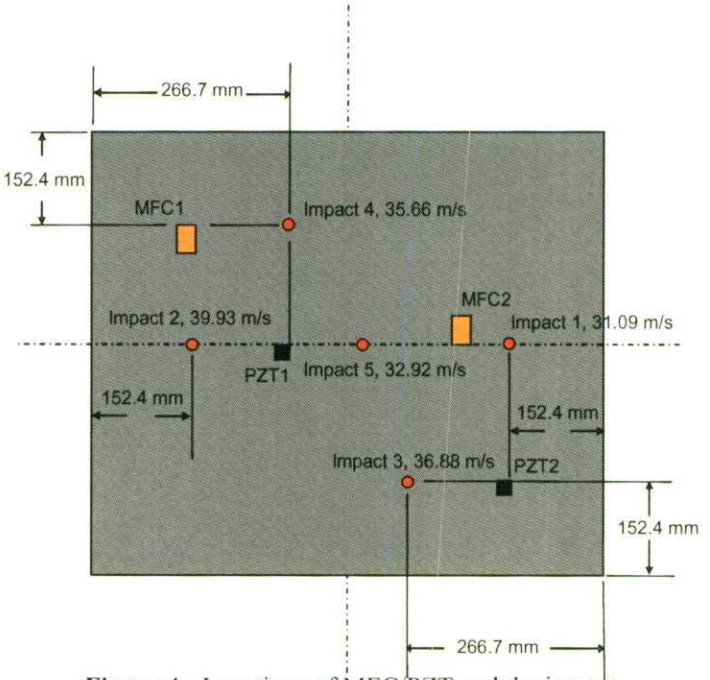

Figure 4: Locations of MFC/PZT and the impact

Experimental Results

Fourteen admittance baseline measurements obtained from PZT 1 and PZT 2 are shown in Figure 5 in the frequency range 0-20 kHz. The temperature variations during the 3 week test period are estimated to be in the range of ± 5 ^{o}C. Several other boundary condition changes are also manually imposed including horizontal and vertical positioning of the plate, suspending the plate with cables to simulate a free-free condition, or resting on soft forms or hard blocks. As can be seen in the Figure, the admittance measurements are quite repeatable. The slope of the admittance remains essentially the same over the 3 week test period when impacts were not induced. It also showed that the admittance measurements are not affected by different structural condition. The slopes of the admittance measured from PZT 1 and PZT 2 are also the same, confirming that the bonding conditions for both PZT sensors are approximately identical.

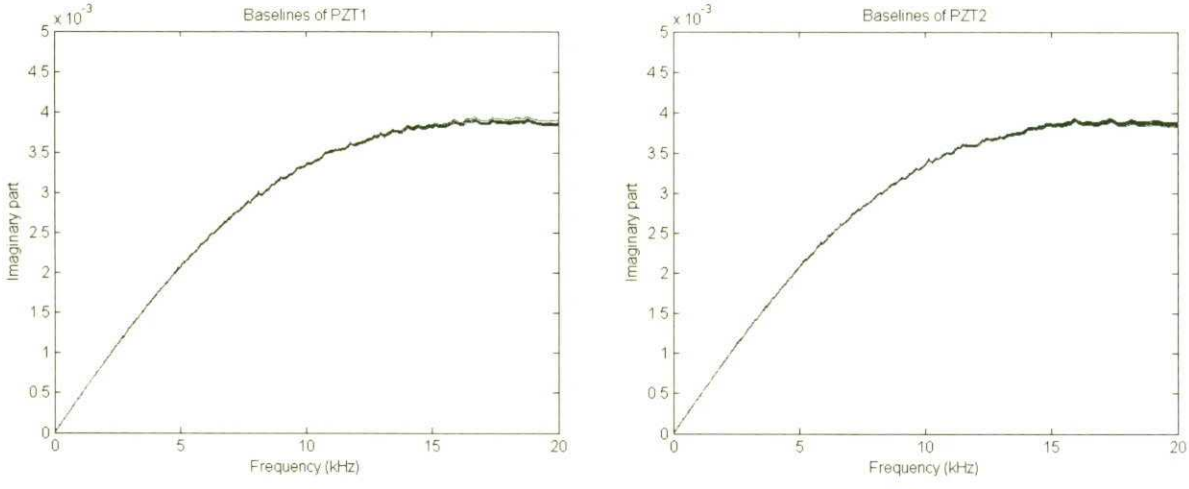

(a) PZT 1 (b) PZT 2

Figure 5: Baseline Admittance Measurements from PZTs

Figure 6 shows the admittance measurement from PZT 1 with induced impacts. When Impact 1 (31.09 m/s) was induced, no change in the response was observed, shown in the first plot in Figure 7, indicating that no damage into the sensor functionality was introduced by Impact 1. Impact 2 (39.93 m/s) produced considerable changes in response, causing a 20% downward shift in the slope. It is believed that, because of the proximity of the PZT 1 and Impact 2, shown in Figure 4, this impact induced an internal fracture to the PZT 1. The measurement taken after Impact 3 did not show any noticeable changes and followed the same pattern as that of Impact 2. After the impact 4, an upward shift of the admittance slope was observed compared to previous readings. This could be considered as an indication of the bonding defects. After several impacts, the integrity of the bonding condition is compromised and the result is an upward shift of the admittance slope. After Impact 5, it has been visually observed that PZT 1 was finally broken, as shown in Figure 7.

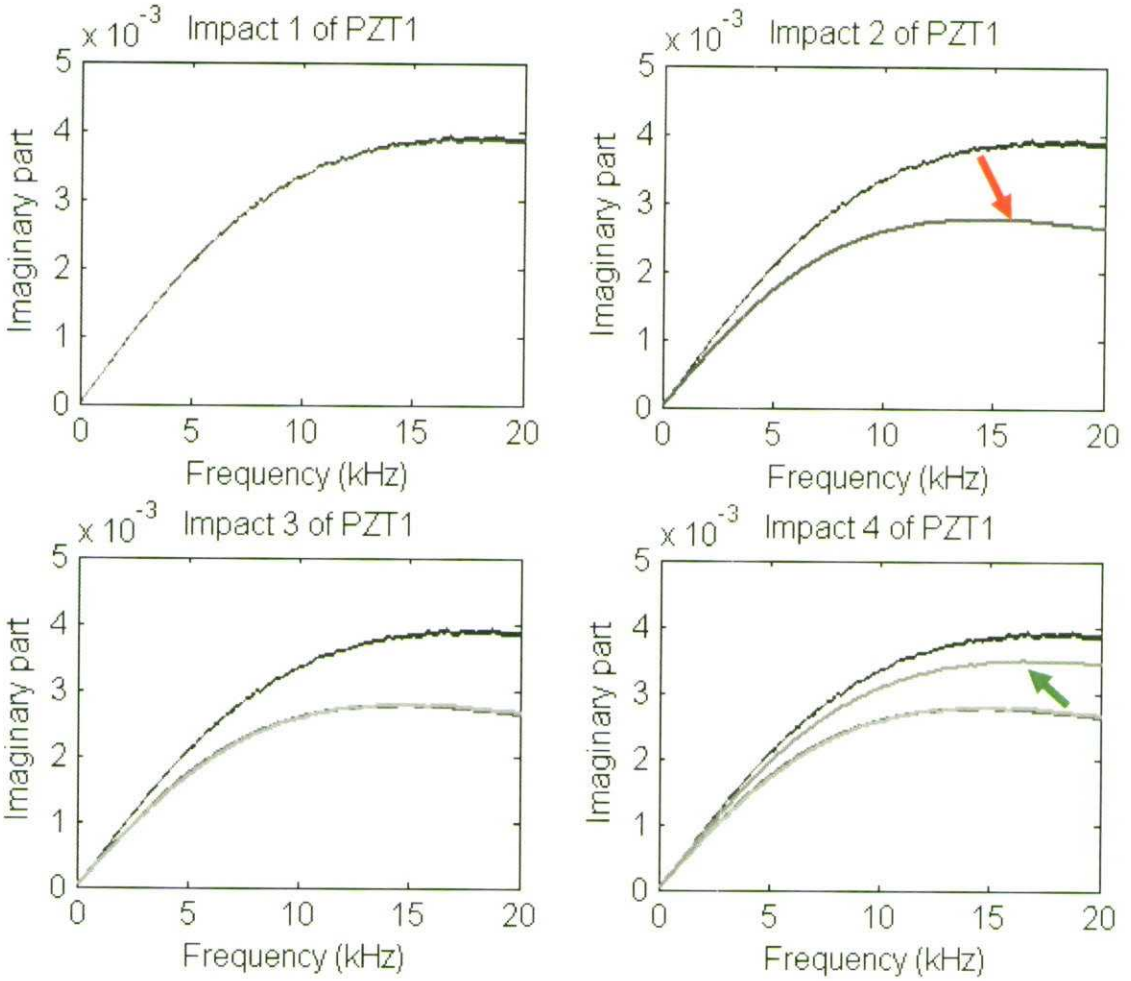

Figure 6: Baselines and Impact responses from PZT 1

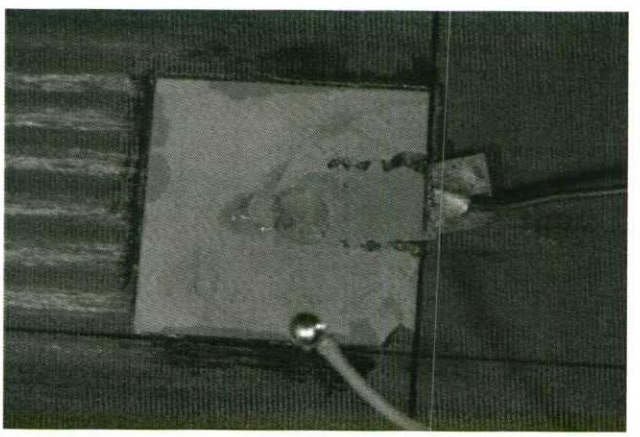

Figure 7: The failure of PZT after Impact 5

The impacts also induced the sensor failure in PZT 2, shown in Figure 8. Impact 1 did not cause any changes, as in the case of PZT 1. A slight upward shift after Impact 2 was

identified, which indicates the degradation in bonding condition. Impact 2, with the highest velocity, obviously causes the sensor breakage of PZT 1 and the bonding defect in PZT 2. Impact 3, which is the closet to the PZT 3, in turn, caused the sensor breakage, shifting the admittance slope downward. Impact 4 shows another slight change, and Impact 5 shows anther an upward shift of the slope, confirming that the bonding condition is continuously deteriorated.

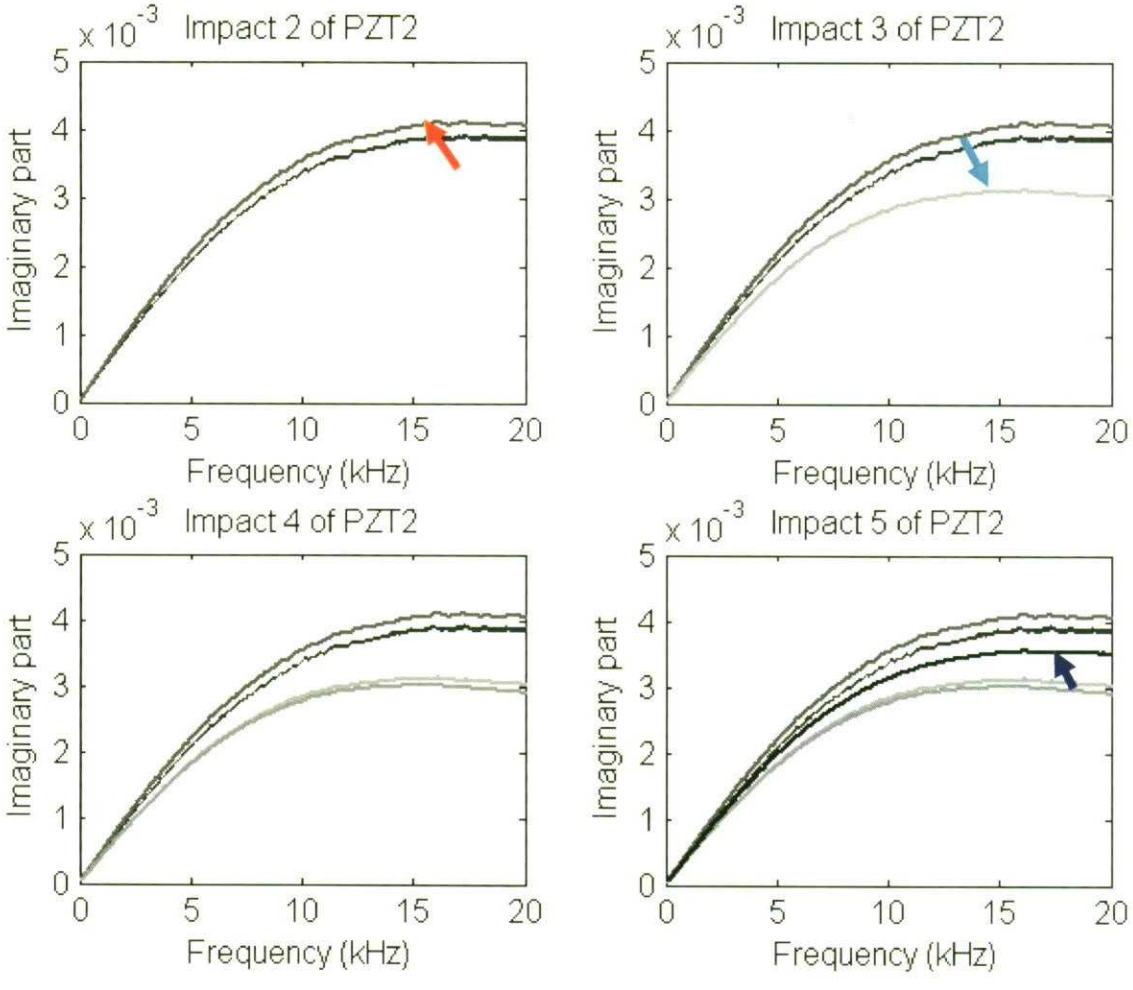

Figure 8: Baselines and Impact responses from PZT 2.

As shown in this section, the imaginary part of the admittance signature provides a unique feature that can be used for sensor diagnostics procedure. The condition of the sensor functionality, including the sensor breakage and the bonding defects, can be assessed by monitoring this feature. It is important to point out that, even with the degraded conditions, the piezoelectric patches were still able to produce sufficient sensing and actuation signals. The measured responses are significantly distorted partially by the induced delamination on the structure, but majority of this changes are believed coming from the sensor failure. This type of sensor failure should be identified before the SHM data processing, if one wants to avoid a false indication regarding the structural health.

On the other hand, MFC sensors provide a superior capability compared to the PZT. Neither of the two MFC sensor's integrity was compromised with the induced impacts. The admittance signatures did not show any noticeable changes. The admittance measurements

before and after the impacts are almost identical, as shown in Figure 9. This flexible sensor certainly provides the advantage of being robust and reliable compared to other available piezoceramic sensors. The MFC sensors are confirmed to be continuously used for monitoring this application by the proposed sensor diagnostic procedure and the SHM results using these MFC sensors can be found in the reference [25].

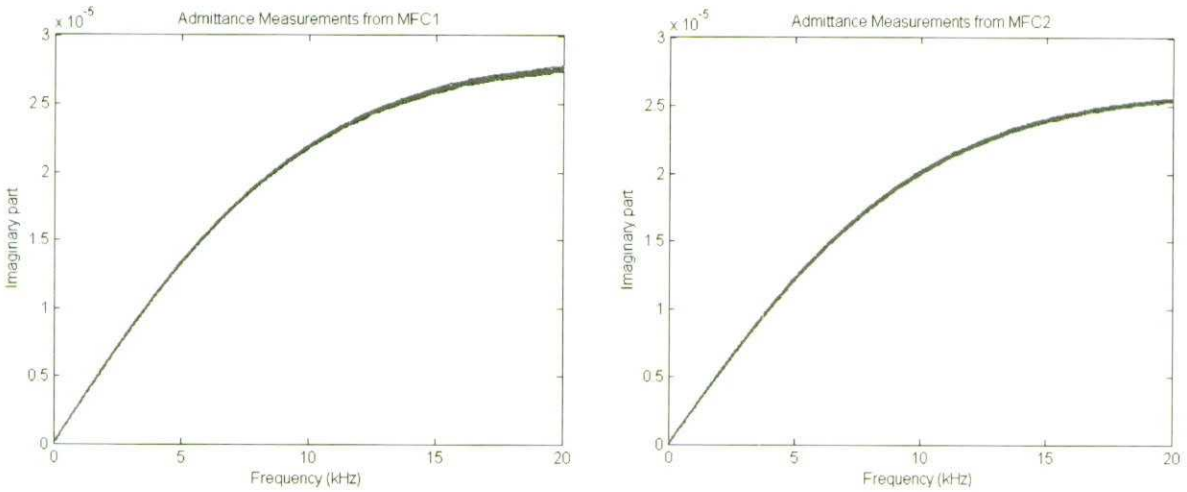

(a) MFC 1 (b) MFC 2

Figure 9: Baselines and Impact responses from MFCs

DISCUSSION

The piezoelectric active sensor self-diagnostic procedure based on the admittance measurements is proposed. While this procedure is efficiently monitor the condition of the sensor functionality, there are still several research issues remained for further investigation.

It is believed that, although the relationship between the sensor breakage and the degree of the downward shift in the admittance slope is quite linear, the bonding defects may not shows up in the linear relation in the admittance measurement. An improved modeling that incorporates the effects of the bonding layer in electrical admittance approximation is required for more quantitative estimation of the bonding defects. This analytical model will also help to identify the sensitivity of the proposed procedure. A more controlled experiment that is able to regulate the degree of sensor failure is required to validate such modeling efforts.

The capacitance of piezoelectric materials is known to be temperature sensitive. A recent study shows that every 5.5 °C change in temperature results in a one percent change in capacitance of the PZT [26]. The automated signal processing that is able to normalize the measured admittance data with respect to varying environmental conditions is essential if one is to fully apply the proposed process. The development of an automated data-processing algorithm to easily interpret the measured admittance signals, coupled with a stand-alone admittance measuring device, is also currently being investigated by authors and these issues are the subjects of the next paper.

CONCLUSION

The piezoelectric sensor self-diagnostic procedure that performs in-situ monitoring of the operational status of piezoelectric sensors and actuators was presented. The basis of this procedure is to track the changes in the measured admittance of piezoelectric materials. Both degradation of the mechanical/electrical properties of the PZT and bonding defects between the PZT and the substructure could be identified using the proposed procedure. The feasibility of the method was demonstrated by an impact testing on a composite plate, where the functionality of surface-mounted piezoelectric sensors was continuously deteriorated. The proposed sensor diagnostic procedure can provide a metric that can be used to determine the sensor functionality over a long period of time or after an extreme loading event.

ACKNOWLEDGEMENT

This research was funded through the Laboratory Directed Research and Development program, entitled "Damage Prognosis Solution," at Los Alamos National Laboratory.

REFERENCE

[1] Crawley, E. F., de Luis, J., 1987. "Use of Piezoelectric Actuators as Elements of Intelligent Structures," *AIAA Journal,* **25**, pp. 1373–1385.

[2] Park, C., Walz, C., Chopra, I., 1996. "Bending and Torsion Models of Beams with Induced-Strain Actuators," *Smart Materials and Structures*, **5**, pp. 98-113.

[3] Sirohi, J., Chopra, I., 2000. "Fundamental Understanding of Piezoelectric Strain Sensors," *Journal of Intelligent Material Systems and Structures*, **11**, pp. 246-257.

[4] Seeley, C.E., Chattopadhyay, A., 1998. "Experimental Investigation of Composite Beams with Piezoelectric Actuation and Debonding," *Smart Materials and Structures*, **7**, pp. 502-511.

[5] Wang, X.D., Meguid, S.A., 2000. "On the Electroelastic Behaviors of a Thin Piezoelectric Actuator Attached to an Infinite Host Structures," *International Journal of Solids and Structures*, **37**, 3231-3251.

[6] Sun, D., Tong, L., Atluri, S.N., 2001. "Effects of Piezoelectric Sensor/Actuator Debonding on Vibration Control of Smart Beams," *International Journal of Solids and Structures*, **38**, pp. 9033-9051.

[7] Tong, L., Sun, D., Atluri, S.N., 2001. "Sensing and Actuation Behaviors of Piezoelectric Layers with Debonding in Smart Beams," *Smart Materials and Structures*, **10**, pp. 713-723.

[8] Rabinovitch, O., Vinson, J.R., 2002. "Adhesive Layer Effects in Surface-mounted Piezoelectric Actuators," *Journal of Intelligent Material Systems and Structures*, **13**, pp. 689-704.

[9] Sun, D.C., Tong, L., 2002. "Control stability analysis of smart beams with debonded piezoelectric actuator layer," *AIAA Journal*, **40**, pp. 1852–1858.

[10] Xu, Y.G., Liu, G.R., 2002. "A Modified Electro-mechanical Impedance Model of Piezoelectric Actuator-sensors for Debonding Detection of Composite Patches," *Journal of Intelligent Material Systems and Structures*, **13**, pp. 389-396.

[11] Faria, A.R., 2003. "The impact of finite-stiffness Bonding on the Sensing Effectiveness o Piezoelectric Patches," *Smart Materials and Structures*, **12**, pp. 5-8.

[12] Sun, D., Tong, L., 2003. "Effect of Debonding in active constrained layer damping patches on hybrid control of smart beams," *International Journal of Solids and Structures*, **40**, pp. 1633-1651.

[13] Bhalla, S., Soh, C.K. 2004. "Electro-Mechanical Impedance Modeling for Adhesively Bonded Piezo-Transducers," *Journal of Intelligent Material Systems and Structures*, in press.

[14] Wu, T., Ro, P.I., 2004. "Dynamic Peak Ampitude Analysis and bonding Layer Effects of Piezoelectric Bimorph Cantilevers," *Smart Materials and Structures*, **13**, 203-210.

[15] Saint-Pierre, N., Jayet, Y., Perrissin-Fabert, I., Baboux, J.C., 1996. "The Influence of Bonding Defects on the Electric Impedance of Piezoelectric Embedded Element," *Journal of Physics D (Applied Physics)*, **29**, pp. 2976-2982.

[16] Giurgiutiu, V., Zagarai, A. Bao, J.J., 2002. "Piezoelectric Wafer Embedded Active Sensors for Aging Aircraft Structural Health Monitoring," *International Journal of Structural Health Monitoring*, **1**, pp. 41-61.

[17] Sun, D., Tong, L., 2003. "Closed-loop Based Detection of Debonding of Piezoelectric Actuator Patches in Controlled Beams," **40**, pp. 2449-2471.
[18] Crawley, E.F., Anderson, E.H., 1990. "Detailed Models of Piezoceramic Actuation of Beams," *Journal of Intelligent Material Systems and Structures*, **1**, pp. 4-25.
[19] Liang, C., Sun, F.P., and Rogers, C.A., 1994. "Coupled Electromechanical Analysis of Adaptive Material System – Determination of Actuator Power Consumption and System Energy Transfer," *Journal of Intelligent Material Systems and Structures,* **5**, pp. 21-20.
[20] Park, G., Sohn, H., Farrar, C.R., Inman, D.J., 2003. "Overview of Piezoelectric Impedance-based Health Monitoring and Path Forward," *The Shock and Vibration Digest,* **35**, pp. 451-463.
[21] Peairs, D., Park, G., Inman, D.J., 2004. "Improving Accessibility of the Impedance-based Structural Health Monitoring Method," *Journal of Intelligent Material Systems and Structures*, **15**, pp. 129-140.
[22] Farrar, C.R., Hemez, F.M., Park, G., Robertson, A., Sohn, H., Williams, T., 2004, "Developing Impact and Fatigue Damage Prognosis Solutions for Composites," *JOM-Journal of Minerals, Metals & Materials Society*, **56**, pp. 40-42.
[23] Wilkie, W.K., Bryant, R.G., High, J.W., Fox, R.L., Hellbaum, R.F., Jalink, A., Little, B.D., Mirick, P.H., "Low-cost piezocomposite actuator for structural control applications," *Proceedings of the 7th SPIE International Symposium on Smart Structures and Materials*, Newport Beach, CA, March 5-9, 2000, SPIE publishing
[24] Sohn, H., Farrar, C.R., 2001. "Damage Diagnosis using Time Series Analysis of Vibration Signals," Smart Materials and Structures, **10**, pp. 446-451
[25] Park, G., Rutherford, C.A., Wait, J.R., Nadler, B.R, Farrar, C.R., 2004, "The Use of High Frequency Response Functions for Composite Plate Monitoring with Ultrasonic Validation," *AIAA Journal*, submitted
[26] Simmers, G.E., Hodgkins, J., Mascarenas, D., Park, G., Sohn, H., 2004. "Improved Piezoelectric Self-sensing Actuation," *Journal of Intelligent Material Systems and Structures*, in press.